

STRUCTURAL, MAGNETIC PROPERTIES AND EXCHANGE-COUPPLING BEHAVIOR OF MAGNETICALLY HARD/SOFT SrFe₁₂O₁₉/Co NANOCOMPOSITE PRODUCED BY THE HIGH ENERGY BALL-MILLING METHOD

^{1,2}Ashraf SEMAIDA, ¹Igor BORDYUZHIN, ¹Pavel MOGILNIKOV, ¹Igor SHCHETININ, ¹Vladimir MENUSHENKOV, ¹Alexander SAVCHENKO

¹National University of Science and Technology MISiS, Moscow, Russian Federation

²Physics Department, Damanhour University, Damanhour, Egypt, amasoud2007@yahoo.com

<https://doi.org/10.37904/metal.2021.4219>

Abstract:

The high energy ball-milling (HEBM) procedure has been used for the preparation of magnetically hard/soft (1-x)SrFe₁₂O₁₉/xCo nanocomposite (with x = 0.1, 0.2 and 0.3). Effects of aging temperatures (800 - 1000 °C) on microstructure, morphology and magnetic properties have been studied. X-ray diffraction spectrum indicates the existence of two phases: the hexagonal SrFe₁₂O₁₉ and Co after HEBM process. Scanning electron microscopy was used to characterize the morphology, size and elemental composition of the synthesized nanocomposites. Thermal gravimetric analysis/differential scanning calorimetry were used to estimate the phase transition temperatures of the nanocomposites. The magnetic characterization was carried out via vibrating sample magnetometer at room temperature for the nanocomposite that showed the magnetically single-phase behavior. With increasing the content of Co, the coercivity (H_c) of the nanocomposites is decreased. Specific saturation magnetization (σ_s) is clearly increased with increasing of aging temperatures until reached the maximum ($\sigma_s = 110 \text{ Am}^2/\text{kg}$) with x = 0.1 aged at 1000 °C. The nanocomposite with x = 0.1 aged at 800 °C has enhancement in the squareness ratio (σ_r/σ_s) that reached to 10.2% increment in comparison with the single phase SrFe₁₂O₁₉. The HEBM process and synthesized SrFe₁₂O₁₉/Co nanocomposite can be regarded as a suitable technique for preparing hard magnetic nanomaterial for permanent magnets.

Keywords: Ball-milling, nanocomposite, SrFe₁₂O₁₉, single-phase

1. INTRODUCTION

Hard/soft magnetic nanocomposites (NCs) have aroused great interest due to the tremendous progress in their magnetic properties [1]. By optimizing the composition, the aging temperature and the appropriate ratio of hard/soft magnetic phases, the structure and magnetic performances of these NCs can be enhanced [2,3]. Hard/soft magnetic NCs were produced using the electrospinning method [4], sol-gel procedure [5] and high energy ball milling (HEBM) process [6, 7]. At the HEBM method, there is a noticeable a “kink” or “bee-waist” at the demagnetization loops, suggesting decoupling between hard and soft phases due to the very large soft-phase grains [7]. In this study, hard/soft (1-x)SrFe₁₂O₁₉/xCo (x = 0.1, 0.2, and 0.3) NCs materials have been synthesized using the HEBM method, with an effort to significantly increase the hard /soft exchange-coupling. The effects of the mass ratio of the hard/soft phases and the aging temperature on the morphology, microstructure and magnetic performances of the hard/soft NCs are discussed.

2. EXPERIMENTAL

Hard/soft (1-x)SrFe₁₂O₁₉/xCo (with x = 0.1, 0.2 and 0.3) NCs was synthesized by the HEBM process. Commercially SrFe₁₂O₁₉ and Co powders of magnetic properties ($H_c = 125, 16.7 \text{ kA/m}$, $\sigma_s = 57.41, 165 \text{ Am}^2/\text{kg}$)

and $\sigma/\sigma_s = 0.441, 0.073$), respectively, were mixed with 2 ml of acetone in a stainless-steel ball mill vial. The Aktivator 2S planetary ball mill was used for milling at a speed of 800 rpm. The sample was milled for 6 hours at room temperature with mass ratio of a ball to powder 10/1. An analogous synthesis process was used to produce other mass ratio composite precursors. Finally, the $(1-x)\text{SrFe}_{12}\text{O}_{19}/x\text{Co}$ composite precursor was aged at 800, 900, and 1000 °C for 2 h, respectively. A Netzsch STA 409 PC/PG thermogravimetric analyser was used for differential scanning calorimetry (DSC)/thermal gravimetric analysis (TGA) measurement. The structure characterization of NCs was carried out by a DRON-4 diffractometer using Co-K α radiation. The morphology and elemental analysis of the powders was achieved using a Bruker Quantax 200 energy dispersive X-ray spectroscopy (EDX). Magnetic measurements were done at room temperature using a vibrating sample magnetometer (VSM-250) under an applied magnetic field up to 1600 kA/m.

3. RESULTS AND DISCUSSION

3.1. X-ray powder diffraction

Figures (1a, b, and c) show the diffraction peaks of the composition, confirming the presence of M-type hexaferrite $\text{SrFe}_{12}\text{O}_{19}$ (SFO) as the hard phase and CoFe_2O_4 spinel ferrite (CFO) as the soft phase.

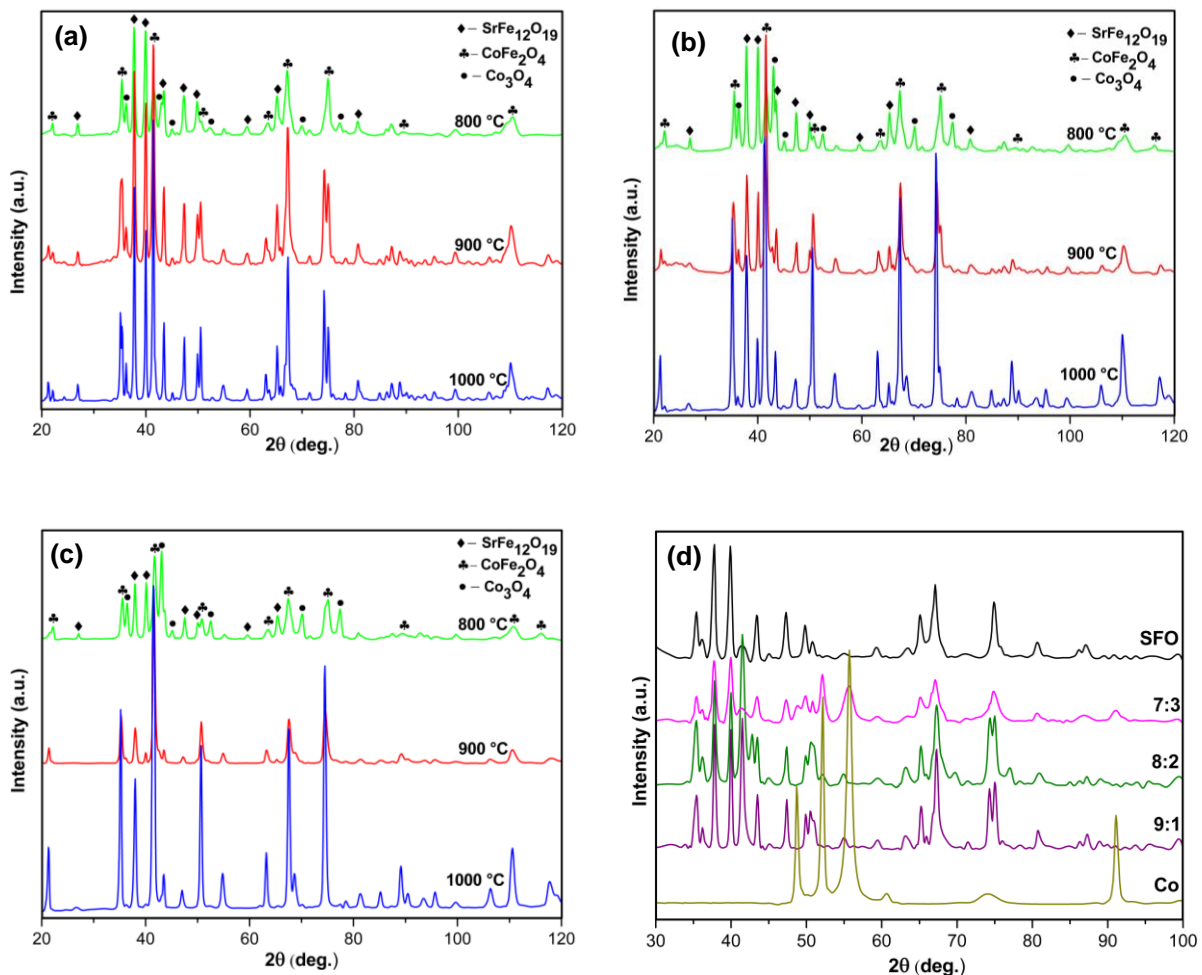


Figure 1 XRD patterns of $(1-x)\text{SrFe}_{12}\text{O}_{19}/x\text{Co}$ composites with different mass ratio of hard/soft ferrites: (a) 9:1, (b) 8:2, (c) 7:3, (d) after ball milling process

Figure 1d indicates the existence of two phases: the hexagonal $\text{SrFe}_{12}\text{O}_{19}$ and Co after HEBM process. As the concentration and aging temperature increase, the diffraction peaks of CFO gradually increase [5]. There is no metal Co peak in the spectrum, indicating that Co ions are located in the crystal sites of the SFO structure and form a CFO phase [8]. At 800 °C, the presence of the Co_3O_4 phase is related to an incomplete aging reaction. When the aging temperature is increased, the occurrence of a high proportion of CFO phase.

The decrease in the relative intensity of the peaks may be due to the substituted ions replacing the occupied ions at the lattice sites. The Co ion preferably occupies the 4f2 and 2a positions of the Fe ion octahedron [9]. As shown in **Table 1**, according to XRD data analysis, the lattice parameters (a and c) and the unit cell volume (V_{cell}) are calculated. Compared with the parent structure ($a = 0.5881$ nm and $c = 2.3052$ nm [8]), the value of the lattice parameter of the SFO phase is increased from $a = 2.3003$ to 2.3076 nm; $c = 0.5873$ to 0.5887 nm with an increase in Co content from 0.1 to 0.3 wt% and increasing aging temperature from 800 to 1000 °C. This increase is attributed to the fact that the ionic radius of the cation Co^{2+} (0.074 nm) is larger than that of Fe^{3+} (0.064 nm) [8]. Due to the increase in a and c , the V_{cell} also increased from 0.6872 to 0.6926 nm³. **Table 1** shows the increase of average crystallite size $\langle D \rangle$, as the aging temperature of all samples was increased from 800 to 1000 °C, demonstrates that grain growth arises during the aging process.

Table 1 Sample composition x , the volume fraction of phases and XRD parameters (the lattice parameter (a , c), the cell volume (V_{cell}) and average crystallite size $\langle D \rangle$ of $\text{SrFe}_{12}\text{O}_{19}$ in $(1-x)\text{SrFe}_{12}\text{O}_{19}/x\text{Co}$ NCs aged at 800, 900 and 1000 °C

x	T (°C)	Phase composition (wt%)				Parameters of $\text{SrFe}_{12}\text{O}_{19}$ phase			
		$\text{SrFe}_{12}\text{O}_{19}$	CoFe_2O_4	Co_3O_4	SrFeO_3	a (nm)	c (nm)	V_{cell} (nm ³)	$\langle D \rangle$ (nm)
0.1	800	71	16	11	2	2.3003	0.5873	0.6872	23.73
	900	62	35	-	3	2.3037	0.5877	0.6891	24.4
	1000	56	40	-	4	2.3045	0.5880	0.6899	34.62
0.2	800	60	18	20	2	2.3027	0.5876	0.6886	19.43
	900	30	58	7	5	2.3048	0.5879	0.6898	22.14
	1000	20	70	-	10	2.3045	0.5881	0.6902	22.31
0.3	800	48	22	27	3	2.3058	0.5882	0.6908	13.52
	900	19	73	-	8	2.3058	0.5884	0.6913	15.14
	1000	5	84	-	11	2.3076	0.5887	0.6926	17.43

3.2. Differential scanning calorimetry

The DSC/TGA analysis of $0.9\text{SrFe}_{12}\text{O}_{19}/0.1\text{Co}$ NCs heated at a rate of 10 °C/min was performed. As illustrated in **Figure 2**, the DSC curve shows a strong endothermic peak near 902 °C. This is due to the transition from Co_3O_4 to CoO and the formation of CFO spinel. The small endothermic peak from 900 to 1100 °C may be due to decomposition of a small amount of $\text{SrFe}_{12}\text{O}_{19}$ and the formation of SrFeO_3 . From the TGA curve, the 2.2% weight loss is mainly caused by the decomposition of Co_3O_4 into CoO and $\text{SrFe}_{12}\text{O}_{19}$ into SrFeO_3 [10].

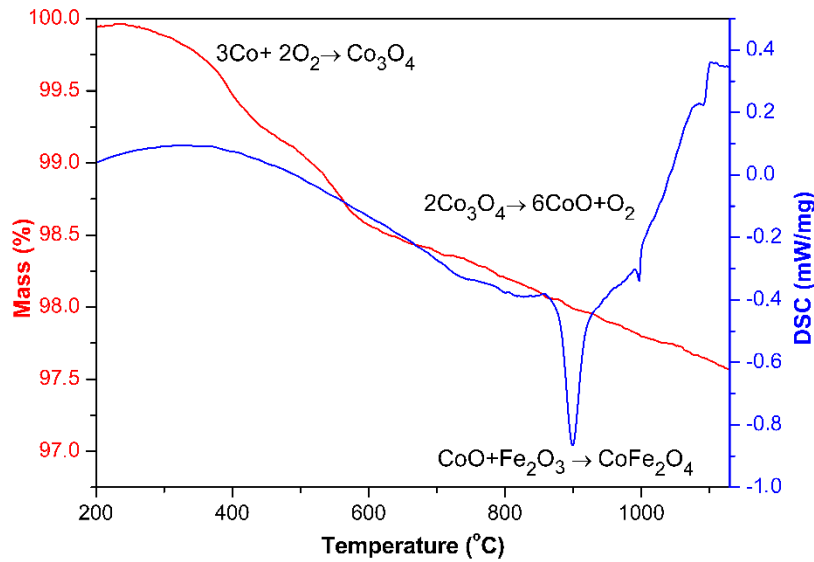


Figure 2 DSC/TGA curves for the formation of CoFe_2O_4

3.3. The morphology

Figure 3 shows SEM image and the results of a representative EDX mapping analysis of $0.9\text{SrFe}_{12}\text{O}_{19}/0.1\text{Co}$ NCs. It can be clearly observed that all relevant elements (Sr, Fe, O and Co) are evenly distributed; confirm that these two phases are evenly distributed in the NC.

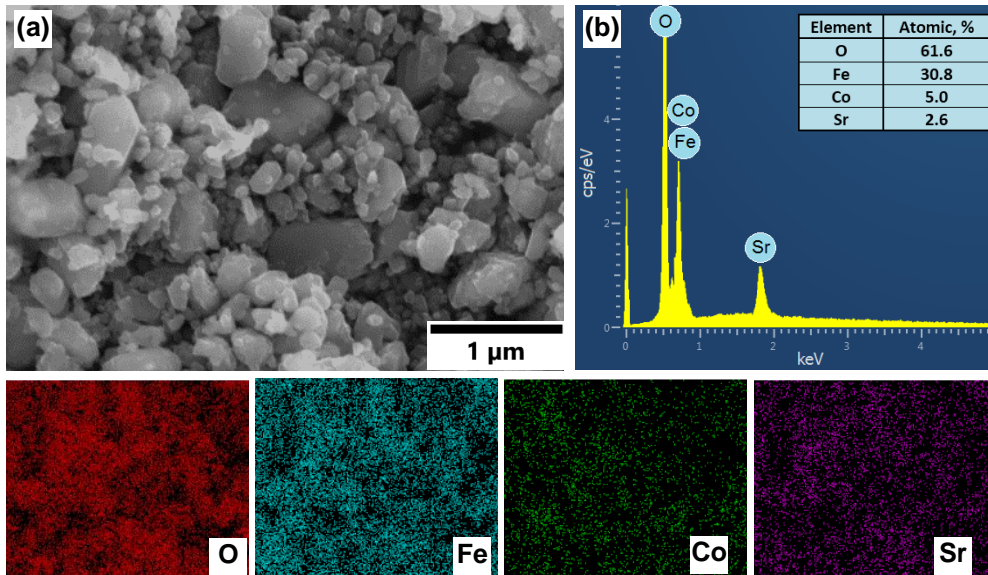


Figure 3(a) SEM image, (b) the EDX spectrum and EDX mapping distribution of O, Fe, Co, and Sr, respectively of the $0.9\text{SrFe}_{12}\text{O}_{19}/0.1\text{Co}$ nanocomposite powders

3.4. Magnetic hysteresis properties

Figure 4 shows the hysteresis loop of $(1-x)\text{SrFe}_{12}\text{O}_{19}/x\text{Co}$ ($x = 0.1, 0.2, 0.3$) NCs at room temperature. The powder sample ($x = 1$) shows hysteresis, indicating that it has hard magnetic properties. However, as the Co content (x) increases, the hysteresis loop becomes smaller, and the magnetization curve shows moderate hard magnetic characteristics at $x = 0.3$, which indicates that the magnetic anisotropy is reduced by the

substitution of $\text{Sr}(\text{Fe},\text{Co})_{12}\text{O}_{19}$. From the smooth demagnetization curve of NCs, an exchange coupled between the magnetically hard/soft phases can be observed [5].

As shown in the **Figure 5a**, the H_c of $(1-x)\text{SrFe}_{12}\text{O}_{19}/x\text{Co}$ ($x = 0.1, 0.2$ and 0.3) decreases monotonously with the increase of x and aging temperature. The $0.1\text{Co}/0.9\text{SrFe}_{12}\text{O}_{19}$ NCs, aged at 800°C , have the maximum H_c (214.9 kA/m); while the $0.3\text{Co}/0.7\text{SrFe}_{12}\text{O}_{19}$ NCs, aged at 1000°C , have the minimum H_c (39.8 kA/m).

This can be attributed to the large crystal grains, it is easy to cause domain wall movement, thus reducing H_c [11]. In addition, as the aging temperature increases, the volume fraction of CFO increases and H_c decreases owing to the fact that the H_c of SFO/CFO NCs is not as large as that of SFO ferrite.

The σ_s of $(1-x)\text{SrFe}_{12}\text{O}_{19}/x\text{Co}$ ($x = 0.1, 0.2$ and 0.3) increases as the calcination temperature increases. In addition, as shown in **Figure 5b**, the σ_s of NCs varies nonlinearly with x . Herein, the $0.9\text{SrFe}_{12}\text{O}_{19}/0.1\text{Co}$ NCs powder, aged at 1000°C , has the highest σ_s value ($110\text{ Am}^2/\text{kg}$). This can be ascribed to the exchange coupled between the magnetically hard/soft phases. Furthermore, the magnetic moment of Co^{2+} ($3\ \mu\text{B}$) is not as large as that of Fe^{3+} ($5\ \mu\text{B}$), so replacing Fe^{3+} with Co^{2+} instead of $4f_2$ will increase the σ_s of the composite material [12]. The $0.7\text{SrFe}_{12}\text{O}_{19}/0.3\text{Co}$ NCs, aged at 800°C , has the lowest σ_s value ($65\text{ Am}^2/\text{kg}$). As the Co substitution increases, the tetrahedral-octahedral exchange interaction between Fe^{3+} and O^{2-} ions weakens, so the magnetic moment value of the system decreases [13].

Remanence (σ_r) of $(1-x)\text{SrFe}_{12}\text{O}_{19}/x\text{Co}$ increases with the increase in aging temperature. As shown in **Figure 5c**, the σ_r trend of $(1-x)\text{SrFe}_{12}\text{O}_{19}/x\text{Co}$ decreases as x increases. Due to the exchange coupled between the magnetically hard/soft phases, σ_r will be generated in the prepared nanocomposite powder.

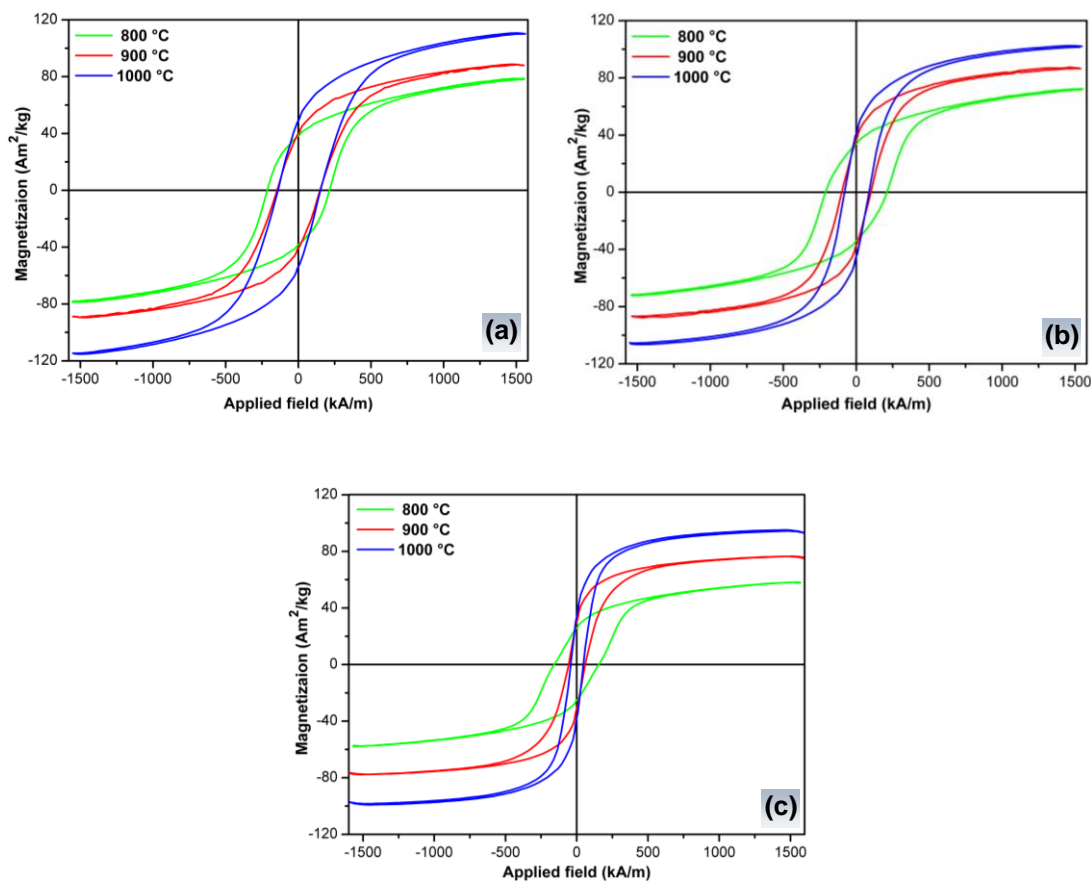


Figure 4 Magnetic hysteresis loops of $(1-x)\text{SrFe}_{12}\text{O}_{19}/x\text{Co}$ composites with different mass ratio of hard/soft ferrites: (a) 9:1, (b) 8:2 and (c) 7:3

The dependence σ_r/σ_s on aging temperature and x is shown in **Figure 5d**. The σ_r/σ_s of $(1-x)$ SrFe₁₂O₁₉/xCo decreased with the increase of aging temperature and showed a nonlinear change with the increase x . The theoretically predictable value of up to 0.50 is attributed to the single domain structure. As the volume fraction of the CFO increases in the NCs, the σ_r/σ_s decreased from 0.489 at 800 °C to 0.352 at 1000 °C. All values of σ_r/σ_s are lower than 0.5, which indicates that all NCs have multi-domain characteristics [2].

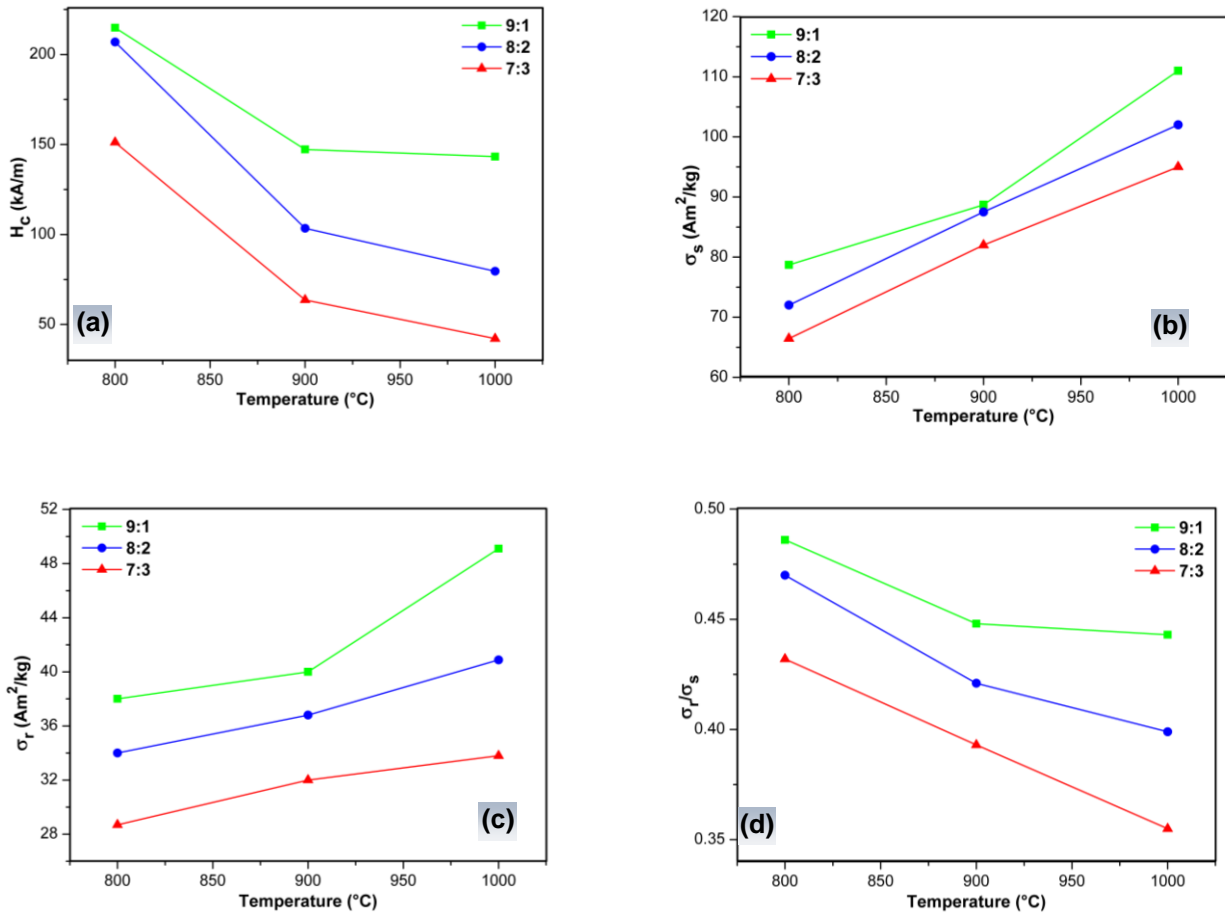


Figure 5 Variation in (a) Coercivity (H_{ci}), (b) specific saturation magnetization (σ_s), (c) remanence (σ_r) and (d) squaresness ratio (σ_r/σ_s) as function of Co content (x) and aging temperature of the $(1-x)$ SrFe₁₂O₁₉/xCoNCs

CONCLUSION

Hard/soft $(1-x)$ SrFe₁₂O₁₉/xCo NCs (with $x = 0.1, 0.2$ and 0.3) was successfully prepared using the HEBM process. The maximum magnetic properties ($H_c = 214.9$ kA/m, $\sigma_s = 82.68$ Am²/kg and $\sigma_r/\sigma_s = 0.489$) were achieved for 0.9SrFe₁₂O₁₉/0.1Co NCs, aged at 800 °C. Excessive Co and higher aging temperature will cause defects in the main hard magnetic SrFe₁₂O₁₉ phase and increase the amount of CoFe₂O₄ soft magnetic phase, thereby reducing the magnetic properties.

Future work will focus on the synthesis of different composites with lower cost and higher performance.

ACKNOWLEDGEMENTS

The work was carried out with financial support from the Ministry of Education and Science of the Russian Federation in the framework of Increase Competitiveness Program of MISiS.

REFERENCES

- [1] SLIMANI, Y. Fabrication of exchange coupled hard/soft magnetic nanocomposites: Correlation between composition, magnetic, optical and microwave properties. *Arabian Journal of Chemistry*. 2021. vol.14, pp. 1-17.
- [2] ALGAROU, N.A. Functional $\text{Sr}_{0.5}\text{Ba}_{0.5}\text{Sm}_{0.02}\text{Fe}_{11.98}\text{O}_4/x(\text{Ni}_{0.8}\text{Zn}_{0.2}\text{Fe}_2\text{O}_4)$ hard-soft ferrite nanocomposites: Structure, magnetic and microwave properties. *Nanomaterials*. 2020. vol.10, pp. 1-18.
- [3] MALTONI, P. Towards bi-magnetic nanocomposites as permanent magnets through the optimization of the synthesis and magnetic properties of $\text{SrFe}_{12}\text{O}_{19}$ nanocrystallites. *Journal of Physics D-Applied Physics*. 2021, vol. 54, pp. 1-10.
- [4] PAN, L.N. A novel method to fabricate $\text{CoFe}_2\text{O}_4/\text{SrFe}_{12}\text{O}_{19}$ composite ferrite nanofibers with enhanced exchange coupling effect. *Nanoscale Research Letters*. 2015, vol. 10, pp. 1-7.
- [5] HARIKRISHNAN, V. , VIZHI, R.E. A study on the extent of exchange coupling between $(\text{Ba}_{0.5}\text{Sr}_{0.5}\text{Fe}_{12}\text{O}_{19})_{1-x}(\text{CoFe}_2\text{O}_4)_x$ magnetic nanocomposites synthesized by solgel combustion method. *Journal of Magnetism and Magnetic Materials*. 2016, vol. 418, pp. 217-223.
- [6] SEMAIDA, A.M. Magnetization performance of hard/soft $\text{Nd}_{9.6}\text{Fe}_{80.3}\text{Zr}_{3.7}\text{B}_{6.4}/\alpha$ -Fe magnetic nanocomposites produced by surfactant-assisted high-energy ball milling. *Materials Research Express*. 2021, vol. 8, pp. 1-11.
- [7] BAJOREK, A. Correlation between microstructure and magnetism in ball-milled SmCo_5/α -Fe (5%wt. α -Fe) nanocomposite magnets. *Materials*. 2021, vol. 14, pp. 1-20.
- [8] CHAKRABORTY, S., BHATTACHARYYA, N.S.,BHATTACHARYYA, S.Effect of Co substitution on absorption properties of $\text{SrCo}_x\text{Fe}_{12-x}\text{O}_{19}$ hexagonal ferrites based nanocomposites in X-band. *Journal of Magnetism and Magnetic Materials*. 2017, vol. 443, pp. 244-251.
- [9] XIE, T.P., XU, L.J.,LIU, C.L.Synthesis and properties of composite magnetic material $\text{SrCo}_x\text{Fe}_{12-x}\text{O}_{19}$ ($x=0-0.3$). *Powder Technology*. 2012, vol. 232, pp. 87-92.
- [10] TANG, C.W., WANG, C.B.,CHIEN, S.H. Characterization of cobalt oxides studied by FT-IR, Raman, TPR and TG-MS. *Thermochimica Acta*. 2008, vol. 473, pp. 68-73.
- [11] TRUKHANOV, A.V. Peculiarities of the magnetic structure and microwave properties in $\text{Ba}(\text{Fe}_{1-x}\text{Sc}_x)_{12}\text{O}_{19}$ ($x < 0.1$) hexaferrites. *Journal of Alloys and Compounds*. 2020, vol. 822, pp. 1-11.
- [12] CHAWLA, S.K. Effect of site preferences on structural and magnetic switching properties of CO-Zr doped strontium hexaferrite $\text{SrCo}_x\text{Zr}_x\text{Fe}_{12-2x}\text{O}_{19}$. *Journal of Magnetism and Magnetic Materials*. 2015, vol. 378, pp. 84-91.
- [13] ZI, Z.F. Effects of Ce-Co substitution on the magnetic properties of M-type barium hexaferrites. *Solid State Communications*. 2012, vol. 152, pp. 894-897.